6º Congreso Argentino de Ingeniería Aeronáutica
VIRTUAL
17, 18 y 19 de Noviembre del 2021

Effects of the cyclic and collective pitch variations on a wind-tunnel rotary-wing decelerator behavior

Juan Francisco Martiarena[1], Vicente Nadal Mora[1], and Joaquín Piechocki[1], Álvaro Cuerva Tejero[2]
Universidad Nacional de La Plata, (1900) La Plata, Buenos Aires, Argentina.

[(1)] *Departamento de Aeronáutica, Facultad de Ingeniería, Universidad Nacional de La Plata.*
[(2)] *Universidad Politécnica de Madrid*

Autor principal: Juan Francisco Martiarena, juanfmartiarena@gmail.com

Key words: Aerodinamics decelerator, dynamics, wind tunnel tests.

The effects of the cyclic and collective pitch variations on a rotating blade decelerator (pararotor) wind-tunnel behavior are studied. The dynamics and aerodynamics effects of the cyclic pitch variations were studied. Starting from the Newton Euler equations, a dynamic model of the main axis dynamics is obtained. The results confirm that the cyclic pitch variations of the blades are an effective way to modify the net force and torque on the pararotor, and consequently, could be used to control pararotors with low aspect ratio blades.

I. Introduction

A pararotor is a rotary wing decelerator that operates in the autorotation regime. During the trimed autorotation phase, both the descent velocity and rotation velocity are constant and the net spin axis aerodynamic torque is zero. The autorotation regime has been well studied in previous works, that have

contributed to establish the fundamentals of the dynamic and aerodynamic behavior of the devices that operate in this regime: Shpund and Levin [1] studied rotating parachutes; Karlsen et. al. [2] worked on winged bodies for submunition applications. Rosen and Seter [3], [4] studied the flight of samara wings. Crimi [5] studied a rotating body with only one wing for submunition applications.

Pararotor devices were developed for atmospheric characterization, atmospherical re-entry systems or projectile guidance and control, and the dynamic and aerodynamic model with a constant collective pitch were well studied [6], [7], [8].

In the present work, the effect of the cyclic pitch on the aerodynamic force on the pararotor is studied. In the present section, the design parameters of the pararotor and the reference systems are defined, in order to obtain a dynamic model for the forces and moments acting on the pararotor by means of the Newton-Euler equations. In section II a theoretical model of the pararotor operating in the wind tunnel is presented. Conclusions are presented in section III, where the main insights are discussed.

Model description

The studied pararotor (see Fig. 1) is modeled as a rigid multibody system composed of a cilindrycal body (indicated with the letter *H*), and two rigid blades (indicated with b=1 and 2) that can pitch an angle θ_b around their span axis, x_{A1b}:

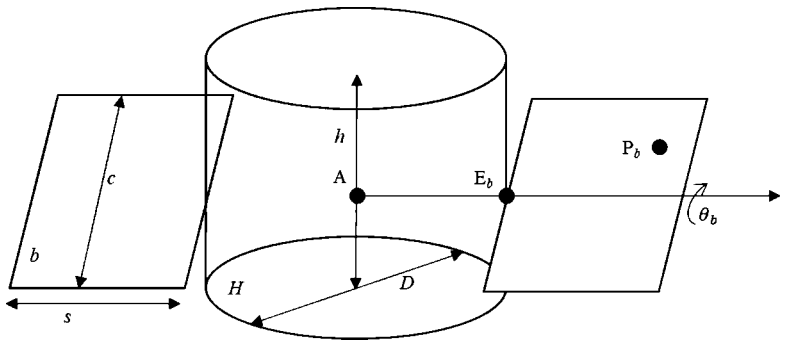

Fig. 1 Pararotor model.

The main rotation axis of the pararotor body is coincident with the main cylinder symmetry axis. The joint between the blade axis and the cilindier is indicated as E_b. The point P_b represents the center of pressure of the blade.

The mass characterization of the body and blades is made by means of their mass M_H and inertial tensor.

The inertial tensor of each element is $\mathbf{I}_H$ for the pararotor body and $\mathbf{I}_b$ for the blades. Each $\mathbf{I}_{ii}$ element of the tensor $\mathbf{I}_H$ is indicated as $\mathbf{I}_j$, with j=1,2,3. The diagonal elements of $\mathbf{I}_b$ are tagged individualy as I_{xB}, I_{yB} and I_{zB}.

II. Theoretical model of the pararotor behavior on the wind tunnel

The Newton-Euler equations for the three mentioned rigid bodies are developed, after considering as external actions: the aerodynamic ones, the gravity one and the coupling forces among the three bodies. Each of the bodies is characterized by its mass, center of mass location and its inertia tensor with respect to axis fixed to the corresponding body. The kinematics of each of the three rigid bodies is characterized by the velocity of the corresponding center of mass and and the angular velocity of the corresponding body.

The Newton-Euler equations give rise to an ordinary differential equation (ODE) system which is presented in the subsection II.B. The ODE system is numerically solved to obtain the angular velocity and a resultant force obtained by a linear combination of the lateral force and the yaw moment in fixed axes generated by the model at the hub reference point.

A. Reference systems

An important issue for the development of the pararotor dynamic equations is to track down the spatial position and attitude of the pararotor. It implies the use of several reference systems, and for the wind-tunnel model we are going to define just those which allows us set up the equation system for this particular case.

Two reference systems fixed to the pararotor body $[x_{1b},y_{1b},z_{1b}]$ are defined with their x_{A1b} axis being coincident with the pitch axis of blade b, the z_{A1b} axis being aligned with the main cylinder symmetry axis, and the y_{A1b} axis forming a right hand defined trihedral. Observe that the rotation plane is defined by axis x_T,z_T or x_{1b},y_{1b} and that axis x_{1b} forms an angle $\psi + (b\text{-}1)\pi$ with axis $-z_T$. Finally, two blade reference systems fixed to each blade, respectively, $[x_{Bb},y_{Bb},z_{Bb}]$, with b = 1, 2, are obtained by rotating the corresponding fixed cylinder reference system $[x_{1b},y_{1b},z_{1b}]$ an angle $\boldsymbol{\theta_b}$ around it axis x_{A1b}. Fig. (**2** shows the body related reference systems. The superscripts are used to indicate the nature and the point where the actions are applied, and the subscripts denotes the reference system used to express the magnitude. For instance, $\boldsymbol{V_{x_{B_b}}^{a,P_b}}$ is the air velocity with respect to point P_b (superscript) in the direction x of the reference system B_b (subscript).

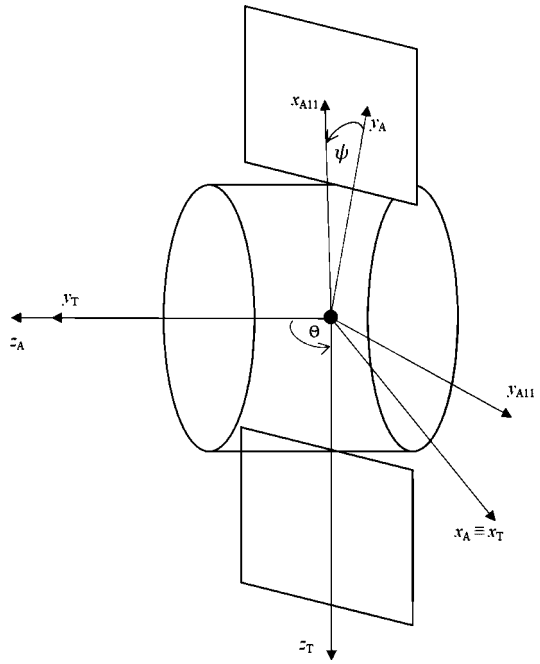

Fig. 2 Scheme of the A and A11 reference systems

¡Error! No se encuentra el origen de la referencia. shows a blade and the forces and moments acting on it. The aerodynamic force $\mathbf{F}_b^a$ is considered to be applied on the center of pressure of the rectangular blade, P_b. The coordinates of this point are indicated by $[x_{Pb},y_{Pb},0]$ in the B_b reference system. The weight of the blade $M_b\mathbf{g}$ is applied on the center of mass (GB_b in the **¡Error! No se encuentra el origen de la**

referencia.), and the reaction force and moment that the cylinder exerts on the connection point E_b, are $\mathbf{F}_b^r$ and $\mathbf{M}_b^{r,E_b}$, respectively.

The velocity of the center of mass of the pararotor body is $\mathbf{V}^{\mathrm{G}} = \mathbf{0}$ and its angular velocity is $\boldsymbol{\omega} = \Omega\mathbf{k}_{\mathrm{A}}$. The absolute velocity of each blade center of mass is $\mathbf{V}^{\mathrm{GB}_b}$, $b = 1, 2$ and $\boldsymbol{\omega}_{\mathrm{b}}$ is its angular velocity. The aerodynamic force on the blade b is decomposed in drag, D_b and lift, L_b components.

The aerodynamic velocity of the pressure center is:

$$\mathbf{V}^{a,\mathrm{P}_b} = -(\mathbf{V}^{\mathrm{E}_b} + \boldsymbol{\omega}_b \wedge \mathbf{E}_b\mathbf{P}_b) + \mathbf{U}_W + \mathbf{v}_i, \tag{1}$$

where

$$\mathbf{V}^{E_b} = \mathbf{V}^G + \boldsymbol{\omega} \wedge \mathbf{GE}_b, \tag{2}$$

and $\mathbf{GE}_{\mathrm{b}}$ is the vector that joins the pararotor body mass center, G, and the blade linkage point E_b.

In Equation (**¡Error! No se encuentra el origen de la referencia.**), the $\mathbf{U}_W$ and $\mathbf{v}_i$ are the wind tunnel flow velocity and the induced velocity, respectively. The air velocity at each blade center of pressure P_b can be expressed in terms of its components in the blade reference system as:

$$\mathbf{V}^{a,P_b} = V_{x_{B_b}}^{a,\mathrm{P}_b}\mathbf{i}_{B_b} + V_{y_{B_b}}^{a,\mathrm{P}_b}\mathbf{j}_{B_b} + V_{z_{B_b}}^{a,\mathrm{P}_b}\mathbf{k}_{B_b}, \tag{3}$$

and is it possible define the angle of attack and the slip angle as:

$$\alpha_b = \tan^{-1}\left[\frac{-V_{z_{B_b}}^{a,P_b}}{\sqrt{\left(V_{x_{B_b}}^{a,P_b}\right)^2 + \left(V_{y_{B_b}}^{a,P_b}\right)^2}}\right], \tag{4}$$

and

$$\beta_b = \tan^{-1}\left[\frac{V_{x_{B_b}}^{a,P_b}}{V_{y_{B_b}}^{a,P_b}}\right], \tag{5}$$

respectively.

The drag and the lift forces are estimated as:

$$L_b = \frac{1}{2}\rho C_L(\alpha_b, \beta_b)|U_r|^2 \tag{6}$$

$$D_b = \frac{1}{2}\rho S C_D(\alpha_b, \beta_b)|U_r|^2,$$

where C_L is the blade lift coefficient and C_D the blade drag coefficient. $U_r = |\mathbf{V}^{a,P_b}|$ is the magnitude of the relative velocity of the air stream to point P_b.

The aerodynamic force, expressed in a wind reference system is defined as:

$$\mathbf{F}_b^a = D_b \mathbf{i}_{B_b} + L_b \mathbf{k}_{B_b}. \tag{7}$$

B. Differential equation system

In the present subsection the mechanical constrains are setted, and the forces acting on the model are analyzed. With those actions a differential equation is obtained.

The wind flow velocity is $\mathbf{U}_W = -U_Z \mathbf{k}_A$, where U_Z is the wind tunnel flow velocity.

The sum of forces and moments transmitted from both blades to the cyilinder are represented as $\mathbf{M}^{t,A}$ and $\mathbf{F}^t$ in Fig. 3. The force $\mathbf{F}^t$ is obtained by adding the aerodynamic, gravitational and inertial forces on the blades, and $\mathbf{M}^{t,A}$ is the moment that results from translating all the forces generated by the blades to point A. It is important to get in mind that each blade presents a pitch angle wich evolves with the azimuth angle ψ as:

$$\theta_b(\psi) = \theta_0(t) + \theta_{1C}(t)\cos[\psi(t) + (b-1)\pi] + \theta_{1S}(t)\sin[\psi(t) + (b-1)\pi] \tag{8}$$

where $\psi_b(t) = \psi(t) + (b-1)\pi$, with b=1,2. In equation (8), θ_0 is the collective pitch angle, and θ_{1C} and θ_{1S} the longitudinal and lateral cyclic pitch angles.

The Newton-Euler equations for the blades are:

$$\mathbf{F}_b^a + \mathbf{F}_b^r + M_b \mathbf{g} = M_b \frac{d\mathbf{V}^{GB_b}}{dt}, \tag{9}$$

$$\mathbf{M}_b^{a,E_b} + \mathbf{M}_b^{r,E_b} + \boldsymbol{E}_b \mathbf{GB}_b \wedge \boldsymbol{M}_b \mathbf{g} = \frac{d\mathbf{h}_b}{dt} + \boldsymbol{E}_b \mathbf{GB}_b \wedge \frac{d\mathbf{V}^{E_b}}{dt}, \tag{10}$$

From equations (9) and (10) it is possible to obtain expressions for the transmitted forces and moments from each blade to the body as $\mathbf{F}_b^t = -\mathbf{F}_b^r$ and $\mathbf{M}_b^{t,E_b} = -\mathbf{M}_b^{r,E_b}$, respectively.

The aerodynamic loads (applied on the point F) exerted by the flow on the pararotor body, $\mathbf{F}_H^{a,\mathrm{F}}$ and $\mathbf{M}_H^{a,\mathrm{F}}$, repectively, are assumed null on a first approach [9].

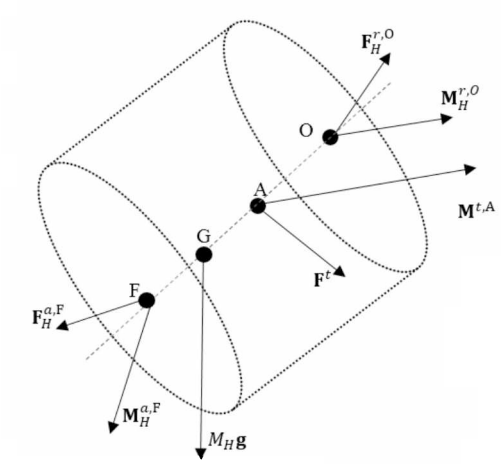

Fig. 3 Forces on the wind tunnel pararotor model.

Observe that in equation (9) and (10) the sum of forces on the pararrotor body is equal to 0, since the center of mass of the pararotor body is fixed in the wind tunnel, and the angular momentum is simply $\mathbf{h}_H = I_3\Omega\mathbf{k}_A$.

The projection of Equation (10) on the $\mathbf{k}_\mathrm{A}$ axis gives the rotational dynamics equation of the model in the wind tunnel:

$$M_{z_A}^{t,\mathrm{A}} - I_3\frac{d\Omega}{dt} = 0, \tag{11}$$

which must be solved simultaneously with the equation

$$\frac{d\psi}{dt} = \Omega \tag{12}$$

where the term $M_{z_A}^{t,\mathrm{A}}$ depends on the azimuth angle ψ.

Equations (11) and (12) shows a nonlinear dependence of several variables. In order to gain insight into the dynamic system formed by latter equations, they are linearized and nondimensionalized.

These considerations lead to obtain a second type Abel differential equation, by replacing the expressions and the Taylor expansion on the system formed by equations (11) and (12):

$$\begin{gathered}\left\{d(1-\cos\psi^2)\theta_{1S}^2 + d\theta_0^2 - 1 - \tfrac{h}{2}\right\}\omega_d(\psi)\tfrac{d\omega_d(\psi)}{d\psi} + \left\{2d(\cos\psi\sin\psi)\theta_{1S}^2 - X_{cp}^3 M\tfrac{C_D}{2}\right\}\omega_d(\psi)^2 - \\ \tfrac{1}{2}X_{cp}^2 M C_{L\alpha}\theta_0\omega_d(\psi) + \tfrac{1}{2}X_{cp}M\left(C_{L\alpha} - \tfrac{C_D}{2}\right) = 0,\end{gathered} \tag{13}$$

Equation (17) is the second order Taylor dimensionless expression, and due to it has no analytical solution [10], it is obtained by means of a numerical implementation on the solver ode45 of MatLab. With the solution of the angular velocity it is possible to obtain the theoretical evolution of $\mathbf{M}^{t,A}$ from equation **¡Error! No se encuentra el origen de la referencia.**, which is useful for the comparison with the experimental results.

For a fixed collective and cyclic pitch angles configuration, a numerical solution of Equation (13) is obtained. As an example, Table 1 shows the general parameters applied for the analysis:

Parameter	Value
$C_{L\alpha}$	0.3 1/rad
C_D	1.44
θ_0	6°
θ_{1S}	0°
U_Z	-5 m/s
I_3	19.15 . 10^{-4} kgm^2
I_{zB}	3.64 . 10^{-4} kgm^2
I_{yB}	3.25 . 10^{-4} kgm^2
ω_{0i}	2

Table 1 Configuration parameters

As it is showed in Fig. 4, the solution for the complete model (the system formed by equations (11) and (12)**¡Error! No se encuentra el origen de la referencia.**) and the solution for the Taylor series model (equation (13)) present minor differences in the angular velocity (in the order of 4%), principally attributed to the second order effects that are not included in the simplified model.

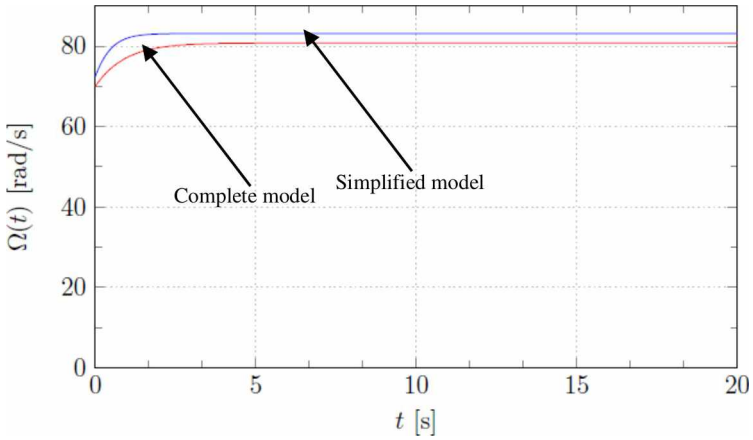

Fig. 4 Angular velocity solution for the case study indicated in table 3.

III. Conclusions

A theoretical model that allows the calculation of the moments produced by a blade cyclic pitch variation on a pararotor mounted inside a wind tunnel was developed from the Newton-Euler equations is obtained..

The theoretical model was developed based on a wind-tunnel model of the behavior of the pararotor. From this model, a Taylor expansion around an equilibrium point and a dimensionless change of variables were applied to obtain a simplified model. This simplified model constitutes an analytical tool to describe the pararotor behavior.

The differences between the complete and simplified models are attributed to the second order effects, which were neglected on the simplified model.

These partial conclusions allow to specify that:

- the cyclic pitch angle variation is a valid strategy to control the moment on the pararotor, giving a way to control the trajectory of the device on free flight, and
- the collective pitch angle has influence on the spin axis dynamics, which is a well known result from the autorotation regime.

Further works would be intended to complete the whole model, without the wind-tunnel restrictions, and validate the model with experimental tests.

References

[1] D. Levin and Z. Shpund, "Dynamic investigation of the angular motion of a rotating body-parachute system," *J. Aircr.*, vol. 32, no. 1, pp. 93–99, 1995.

[2] D. Borgstrom, L. Paulsson, and L. Karlsen, "Aerodynamics of a rotating body descending from the separation position of an artillery munition shell," in *11 th Aerodynamic Decelerator Systems Technology Conference. San Diego, CA, US: AIAA*, 1991.

[3] D. Seter and A. Rosen, "Stability of the vertical autorotation of a single-winged samara," *J. Appl. Mech.*, vol. 59, no. 4, pp. 1000–1008, 1992.

[4] A. Rosen and D. Seter, "Vertical autorotation of a single-winged samara," *J. Appl. Mech.*, vol. 58, no. 4, pp. 1064–1071, 1991.

[5] P. Crimi, "Analysis of samara-wing decelerator steady-state characteristics," *J. Aircr.*, vol. 25, no. 1, pp. 41–47, 1988.

[6] V. J. Nadal Mora, "Comportamiento aerodinámico de sondas atmosféricas en entornos aeroportuarios," ETSI Aeronauticos, 2005.

[7] J. Piechocki, "Estudio de la Dinámica del Vuelo de un Decelerador Aerodinámico Basado en el Concepto de Pararrotor," Facultad de Ingenier\'\ia, UNLP, 2012.

[8] J. F. Martiarena, V. N. Mora, and J. Piechocki, "Experimental study of the effect of blade curvature and aspect ratio on the performance of a rotary-wing decelerator," *Aerosp. Sci. Technol.*, vol. 43, pp. 471–477, 2015.

[9] J. Martiarena, "Estudio del desplazamiento lateral de un decelerador de alas rotatorias de pequeño alargamiento a través de las variaciones c{\'\i}clicas del paso de las palas," Facultad de Ingenier{\'\i}a, 2018.

[10] V. F. Zaitsev and A. D. Polyanin, *Handbook of exact solutions for ordinary differential equations*. CRC press, 2002.

[11] BIPM, "Evaluations of measurement data - Guide to the expression of uncertainty in measurement.," 2008.